Structure, Reactivity, and an EHMO Analysis of a Metal-Stabilized Dicarbenium Ion, $[Cp_2Mo_2(CO)_4(CH_2CCCH_2)][BF_4]_2$

Mark D. McClain, Michael S. Hay, M. David Curtis,* and Jeff W. Kampf

Willard H. Dow Laboratories, Department of Chemistry, The University of Michigan, Ann Arbor, Michigan 48109-1055

Received May 23, 1994[⊗]

Treatment of $Cp_2Mo_2(CO)_4(HOCH_2C{\equiv}CCH_2OH)$ (**1a**) with $HBF_4{\cdot}Et_2O$ in CH_2Cl_2 produced $[Cp_2Mo_2(CO)_4(CH_2CCCH_2)][BF_4]_2$ (**2**·$[BF_4]_2$) which was recrystallized from MeCN and structurally characterized. The dication **2**·$[BF_4]_2$ crystallizes in the monoclinic space group $P\bar{1}$ (No. 2) with cell dimensions $a = 9.779(1)$ Å, $b = 10.982(3)$ Å, $c = 12.680(3)$ Å, $\alpha = 103.09(2)°$, $\beta = 93.04(2)°$, $\gamma = 92.16(2)°$, $V = 1322.8(5)$ Å^3, and $Z = 2$. Diffraction data were collected at −97 °C, and the structure was refined to $R = 3.2\%$ and $R_w = 5.2\%$ for those unique 5906 data with $F_o \geq 0.6\sigma(F)$. The title compound was found to undergo nucleophilic addition with $(^iPr)_2NH$ and MeOH, but reduction with Na/Hg did not produce oligomers cleanly. "Masked" dicarbenium ions, $Cp_2Mo_2(CO)_4(MeCO_2CH_2C{\equiv}CCH_2O_2CMe)$ and $[Cp_2Mo_2(CO)_4(LCH_2C{\equiv}CCH_2L)][BF_4]_2$ (L = *tert*-butylpyridine), were found to undergo limited substitution. An EHMO analysis of the structure and reactivity of **2** and a moncarbenium ion complex, $Cp_2Mo_2(CO)_4(HCCCH_2)^+$, is presented. These calculations indicate that all the positive charge of the "carbenium" ion is transferred to the metal atoms, and the regioselectivity of the reactions with nucleophiles is frontier-orbital controlled.

Introduction

Carbenium ions stabilized by metal dimers (M_2L_6) have been mainly studied for their synthetic utility in alkyne functionalization (Nicholas reaction[1] for ML_3 = $Co(CO)_3$) and their fluxionality in solution.[2-10] Thus far, X-ray structural studies have only given insight into the nature of the stabilization for $ML_3 = MoCp(CO)_2$[4,9-14] or $WCp(CO)_2$.[15] Though dicarbenium ions stabilized by Co[16-20] or Mo[17,21] have been described, no structural information is known. This article reports the first structural characterization and EHMO analysis of a metal-stabilized dicarbenium ion, $[Cp_2Mo_2(CO)_4(CH_2CCCH_2)][BF_4]_2$ (**2**·$[BF_4]_2$), and a comparison of its structure and reactivity with monocarbenium salts.

Experimental Section

General Considerations. All reactions were performed under nitrogen on a Schlenk line or in a glovebox. All solvents were distilled from appropriate drying agents: sodium benzophenone ketyl (toluene, diglyme, diethyl ether, THF) or calcium hydride (dichloromethane, acetonitrile, hexane, diisopropylamine). $HBF_4{\cdot}Et_2O$ and $HOCH_2C{\equiv}CCH_2OH$ were obtained from Aldrich and used as received. NMR spectra were collected on a Bruker WM360 or AM300. IR spectra were collected on a Nicolet DX-5B. Mass spectra were collected on a VG 70-250-S high-resolution spectrometer. Elemental analyses were performed at the University of Michigan Microanalysis Laboratory.

Preparation of $Cp_2Mo_2(CO)_4(ROCH_2C{\equiv}CCH_2OR)$ (1) (R = H,[22] Me). 1a: A toluene solution (150 mL) of $Cp_2Mo_2(CO)_4$[23] (5.00 g, 11.5 mmol) and $HOCH_2C{\equiv}CCH_2OH$ (0.992 g, 11.5 mmol) in a 500 mL Schlenk flask was stirred for 24 h. To redissolve all the product, CH_2Cl_2 (100 mL) was added and

[⊗] Abstract published in *Advance ACS Abstracts,* October 1, 1994.

(1) Nicholas, K. M. *Acc. Chem. Res.* **1987**, *20*, 207–214 and references therein.
(2) Padmanabhan, S.; Nicholas, K. M. *J. Organomet.Chem.* **1984**, *268*, C23–C27.
(3) Schreiber, S. L.; Klimas, M. T.; Sammakia, T. *J. Am. Chem. Soc.* **1987**, *109*, 5749–5759.
(4) Meyer, A.; McCabe, D. J.; Curtis, M. D. *Organometallics* **1987**, *6*, 1491–1498.
(5) Troitskaya, L. L.; Sokolov, V. I.; Bakhmutov, V. I.; Reutov, O. A.; Gruselle, M.; Cordier, C.; Jaouen, G. *J. Organomet. Chem.* **1989**, *364*, 195–206.
(6) D'Agostino, M. F.; Frampton, C. S.; McGlinchey, M. J. *J. Organomet. Chem.* **1990**, *394*, 145–166.
(7) Cordier, C.; Gruselle, M.; Jaouen, G.; Bakhmutov, V. I.; Galakhov, M. V.; Troitskaya, L. L.; Sokolov, V. I. *Organometallics* **1991**, *10*, 2303–2309.
(8) Galakhov, M. V.; Bakhmutov, V. I.; Barinov, I. V.; Reutov, O. A. *J. Organomet. Chem.* **1991**, *421*, 65–73.
(9) Cordier, C.; Gruselle, M.; Vaissermann, J.; Troitskaya, L. L.; Bakhmutov, V. I.; Sokolov, V. I.; Jaouen, G. *Organometallics* **1992**, *11*, 3825–3832.
(10) El Amouri, H.; Vaissermann, J.; Besace, Y.; Vollhardt, K. P. C.; Ball, G. E. *Organometallics* **1993**, *12*, 605–609.
(11) Gruselle, M.; Cordier, C.; Salmain, M.; El Amouri, H.; Guerin, C.; Vaissermann, J.; Jaouen, G. *Organometallics* **1990**, *9*, 2993–2997.
(12) Barinov, I. V.; Reutov, O. A.; Polyakov, A. V.; Yanovsky, A. I.; Struchkov, Y. T.; Sokolov, V. I. *J. Organomet. Chem.* **1991**, *418*, C24-C27.
(13) Le Berre-Cosquer, N.; Kergoat, R.; L'Haridon, P. *Organometallics* **1992**, *11*, 721–728.
(14) Gruselle, M.; El Hafa, H.; Nikolski, M.; Jaouen, G.; Vaissermann, J.; Li, L.; McGlinchey, M. J. *Organometallics* **1993**, *12*, 4917–4925.
(15) Froom, S. F. T.; Green, M.; Nagle, K. R.; Williams, D. J. *J. Chem. Soc., Chem. Commun.* **1987**, 1305–1307.
(16) Bennett, S. C.; Phipps, M. A.; Went, M. J. *J. Chem. Soc., Chem. Commun.* **1994**, 225–226.
(17) Bennett, S. C.; Gelling, A.; Went, M. J. *J. Organomet. Chem.* **1992**, *439*, 189–199.
(18) Gelling, A.; Mohmand, G. F.; Jeffery, J. C.; Went, M. J. *J. Chem. Soc., Dalton Trans.* **1993**, 1857–1862.
(19) Takano, S.; Sugihara, T.; Ogasawara, K. *Synlett.* **1992**, 70–72.
(20) Buchmeiser, M.; Schottenberger, H. *Organometallics* **1993**, *12*, 2472–2477.
(21) Reutov, O. A.; Barinov, I. V.; Chertkov, V. A.; Sokolov, V. I. *J. Organomet. Chem.* **1985**, *297*, C25–C29.
(22) Cluster **1a** has been prepared previously without full characterization.[17,21]
(23) Curtis, M. D.; Fotinos, N. A.; Messerle, L.; Sattelberger, A. P. *Inorg. Chem.* **1983**, *22*, 1559–1561.

0276-7333/94/2313-4377$04.50/0

the solution filtered through Celite (3 × 4 cm). The filtrate was concentrated *in vacuo* with warming (45 °C) and cooled to room temperature. Crystallization was completed in a freezer (−20 °C). Dark red crystals were collected by filtration and rinsed with hexane. Yield: 5.24 g, 87%. IR (toluene, cm^{-1}): ν(C≡O) 1987 (s), 1911 (s), 1840 (s). ^1H NMR (C_6D_6): δ 4.89 (s, 10 H Cp), 4.75 (d, 4 H, CH_2OH, J = 4.7 Hz), 2.79 (t, 2 H, CH$_2$OH, J = 4.7 Hz). $^{13}C\{^1H\}$ NMR (C_6D_6): δ 230.1 (C≡O), 91.3 (Cp), 83.7 (CH$_2$$CCCH_2$), 67.6 ($CH_2$OH). Anal. Calcd for $C_{18}H_{16}Mo_2O_6$: C, 41.56; H, 3.10. Found: C, 41.32; H, 2.84.

1b: Prepared as described for **1a** except MeOCH$_2$C≡CCH$_2$OMe[24] was used as the alkyne. Yield: 65%. IR (toluene, cm^{-1}): ν(C≡O) 1996 (s), 1910 (s), 1839 (s). ^1H NMR (C_6D_6): δ 4.99 (s, 10 H Cp), 4.57 (s, 4 H, CH_2OMe), 3.19 (s, 6 H, Me). $^{13}C\{^1H\}$ NMR (C_6D_6): δ 230.1 (C≡O), 91.2 (Cp), 80.8 (CH$_2$$CCCH_2$), 77.8 ($CH_2$OMe), 58.6 (Me). Anal. Calcd for $C_{20}H_{20}Mo_2O_6$: C, 43.82; H, 3.68. Found: C, 43.48; H, 3.41.

Preparation of $Cp_2Mo_2(CO)_4(CH_2CCCH_2)(BF_4)_2$ (2·[BF$_4$]$_2$). To a stirred solution of **1a** (5.5 g, 10.6 mmol) in CH_2Cl_2 (150 mL) in a 500 mL Schlenk flask was added dropwise HBF_4·Et_2O (4.0 mL of a 85% ether solution). A red precipitate formed, leaving a light orange solution. The supernatant liquid was removed *via* cannula and the residue rinsed with ether (30 mL) and THF (30 mL) and evacuated to dryness, yielding 6.4 g (92%) of product. The solid was recrystallized from CH_3CN at −20 °C to yield $Cp_2Mo_2(CO)_4(CH_2C{\equiv}CCH_2)(BF_4)_2(MeCN)_2$ as orange parallelepipeds. IR (KBr, cm^{-1}): ν(C≡O) 2043 (s), 2015 (vs), 1976 (vs), 1911 (m). ^1H NMR and $^{13}C\{^1H\}$ NMR (CD_3CN) data agree with reported values.[21] Anal. Calcd for $C_{22}H_{20}B_2F_8Mo_2N_2O_4$: C, 35.62; H, 2.72; N, 3.78. Found: C, 35.77; H, 2.66; N, 3.78.

Preparation of $Cp_2Mo_2(CO)_4(\mu$-(^{i}Pr)$_2$NCH$_2$C≡CCH$_2$N(^{i}Pr)$_2$) (5). Dry, distilled diisopropylamine (10 mL) was transferred *via* cannula into a 25 mL round bottom flask containing **2**·[BF$_4$]$_2$(MeCN)$_2$ (0.230 g, 0.31 mmol). The solution became red slowly as the solid dissolved. After 2 h, dry acetonitrile (5 mL) was added to completely dissolve the remaining dication. The solution was stirred overnight for 16 h and the solvent was removed *in vacuo*. The residue was extracted with hexane (10 mL) and filtered through Celite (1 cm) in a Pasteur pipet. The solvent was allowed to evaporate in a glovebox, yielding a red solid: 0.165 mg, 78%. IR (CH_2Cl_2, cm^{-1}): ν(C≡O) 1973 (s), 1936 (sh), 1903 (vs), 1821 (m). ^1H NMR (C_6D_6): δ 5.17 (s, 10 H Cp), 4.15 (s, 4 H, CH$_2$), 3.16 (septet, 4 H, CH, J = 6.6 Hz), 1.07 (d, 24 H, CH$_3$). $^{13}C\{^1H\}$ NMR (C_6D_6): δ 232.1 (C≡O), 90.7 (Cp), 51.7 (CH$_2$), 47.0 (CH), 20.8 (CH$_3$). Anal. Calcd for $C_{30}H_{42}Mo_2N_2O_4$: C, 52.48; H, 6.17; N, 4.08. Found: C, 52.78; H, 6.18; N, 3.87. MS (DCI): *m/e* 686, $[M]^+$.

Reaction of 2·[BF$_4$]$_2$(MeCN)$_2$ with MeOH. Anhydrous MeOH (15 mL) was transferred *via* cannula into a 100 mL round bottom flask containing **2**·[BF$_4$]$_2$(MeCN)$_2$ (0.102 g, 0.137 mmol). The solution became orange-red slowly as some of the solid dissolved. With addition of 2,6-lutidine (0.20 mL, 1.7 mmol), the solution became redder. After stirring at 50 °C for 1 h, the solvent was removed *in vacuo*. The residue was extracted with toluene (2 × 15 mL) and filtered through Celite (2 × 4 cm). Upon removal of the solvent under vacuum, the residue was shown by ^1H NMR to be >90% **1b**.

Reaction of 2·[BF$_4$]$_2$(MeCN)$_2$ with Na/Hg. A solution of **2**·[BF$_4$]$_2$(MeCN)$_2$ in MeCN was stirred over Na/Hg amalgam for periods up to 2 weeks. Several reaction attempts were made, resulting in little or no reactivity when 2 equiv of Na/cluster was employed. When a large excess of Na was used, many lines in the Cp region of the ^1H NMR spectrum were seen and several low-frequency CO stretching bands were observed.

Reaction of $Cp_2Mo_2(CO)_4$ with ClCH$_2$C≡CCH$_2$Cl. Degassed 1,4-dichloro-2-butyne (over 4 Å sieves) (0.11 mL, 1.12 mmol) was added to a stirred solution of $Cp_2Mo_2(CO)_4$ (0.50 g, 1.15 mmol) in toluene (40 mL). The solution was stirred at Room temperature for 24 h. Solution IR indicated the presence of $Cp_2Mo_2(CO)_6$ and $CpMo(CO)_3Cl$.[25] The solution was filtered through Celite (4 × 3 cm) to remove a large quantity of black solid, and the solvent was removed *in vacuo*. ^1H NMR (C_6D_6) peaks of δ 4.67 and 4.63 indicated small amounts of $Cp_2Mo_2(CO)_6$ and $Cp_2Mo_2(CO)_4$, with the major signal due to the $CpMo(CO)_3Cl$ (δ(Cp) = 5.43).

Preparation of $Cp_2Mo_2(CO)_4$(MeCO$_2$CH$_2$C≡CCH$_2$O$_2$CMe) (6). Nitrogen was bubbled through acetic anhydride (40 mL) in a 250 mL Schlenk flask for 20 min. Compound **1a** (1.5 g, 2.9 mmol) was added under flowing nitrogen and the solution vacuum degassed three times. The dark red solution developed an orange-red cast upon stirring for 3 h. The produced acetic acid and excess anhydride were removed *in vacuo* to yield a red oil. The residue was crystallized from CH_2Cl_2/hexane to yield large crystals of $Cp_2Mo_2(CO)_4$(MeCO$_2$CH$_2$C≡CCH$_2$O$_2$CMe). Total yield: 1.45 g, 83%. IR (KBr, cm^{-1}): ν(C≡O) 1986 (s), 1931 (s), 1906 (vs), 1824 (s); ν(C=O) 1728 (m). ^1H NMR (C_6D_6): δ 5.42 (s, 4 H, CH_2); 4.85 (s, 10 H, Cp), 1.76 (s, 6 H, Me). $^{13}C\{^1H\}$ NMR (C_6D_6): δ 229.2 (C≡O), 169.9 (C=O), 91.0 (Cp), 78.2 (C≡C), 69.5 (CH$_2$), 20.3 (Me). Anal. Calcd for $C_{22}H_{22}Mo_2O_8$: C, 43.73; H, 3.34. Found: C, 43.50; H, 3.34. FAB MS (*m/e*): 604, $[M]^+$; 545, [M − acetate]$^+$; 433, [M − acetate-4CO]$^+$. This compound was found to be identical to that prepared from $Cp_2Mo_2(CO)_4$ and MeCO$_2$CH$_2$C≡CCH$_2$O$_2$CMe.

Reaction of 6 with PhCOOH. Compound **6** (0.11 g, 0.18 mmol) and benzoic acid (46 mg, 0.38 mmol) were placed in a 100 mL Schlenk flask which was evacuated/back-filled with nitrogen (3×). Diglyme (30 mL) was added and the solution stirred at 60 °C for 2 h. The solvent was removed *in vacuo*, yielding a red solid. ^1H NMR (C_6D_6) showed benzoic acid with an inseparable mixture of 75% $Cp_2Mo_2(CO)_4$(PhCO$_2$CH$_2$C≡CCH$_2$O$_2$CPh) [δ 8.2 (m, 4 H, ring), 7.0 (m, 6 H, ring), 5.76 (s, 4 H, CH_2), 4.88 (s, 10 H, Cp)] and 25% $Cp_2Mo_2(CO)_4$(MeCO$_2$CH$_2$C≡CCH$_2$O$_2$CPh) [δ 8.2 (m, 2 H, ring), 7.0 (m, 3 H, ring), 5.69 (s, 2 H, CH_2), 5.48 (s, 2 H, CH_2), 4.87 (s, 10 H, Cp), 1.73 (s, 3 H, Me)].

Reaction of 6 with LiOMe. A solution of LiOMe (0.35 mmol) in MeOH was added to a stirred solution of **6** (0.11 g, 0.18 mmol) in MeOH (5 mL). After 1 h, the solution became much redder and the solvent was removed *in vacuo*. ^1H NMR (C_6D_6) showed 90% conversion to **1b**.

Reaction of 2·(4-^{t}BuPy)$_2$[CF$_3$CO$_2$]$_2$. Nitrogen was bubbled through trifluoroacetic anhydride (10 mL) in a 100 mL Schlenk flask for 20 min. Compound **1a** (1.5 g, 2.9 mmol) was added under flowing nitrogen and the solution vacuum degassed three times. The dark red solution developed an orange-red cast upon stirring for 1 h. The volatiles were removed *in vacuo* to yield an orange-red oil. ^1H NMR (CD_3CN), δ 5.64 (Cp), suggested a monocation in solution.[21] The residue was rinsed with Et_2O and 4-*tert*-butylpyridine (^{t}BuPy) (1.0 mL, 6.8 mmol) was added after dissolution in MeCN, resulting in a red solution upon stirring for 2 h. The red powder which remained when the solvent was removed under vacuum was rinsed with Et_2O and dried *in vacuo*. ^1H NMR (acetone-d_6): δ 9.31 (d, 4 H, ring, J = 5.8 Hz), 8.36 (d, 4 H, ring, J = 5.8 Hz), 6.29 (s, 4 H, CH$_2$), 5.45 (s, 10 H, Cp), 1.45 (s, 18 H, CMe$_3$). $^{13}C\{^1H\}$ NMR (acetone-d_6): δ 234.0 (C≡O); 172.6, 146.1, 126.2 (ring); 92.1 (C≡C); 90.0 (Cp); 67.9 (CH$_2$); 37.3 (CMe$_3$); 30.0 (Me).

Reaction of 2·(4-^{t}BuPy)$_2$[CF$_3$CO$_2$]$_2$ with MeOH. MeOH (15 mL) and **2**·(4-^{t}BuPy)$_2$[CF$_3$CO$_2$]$_2$ (50 mg) were stirred in a 25 mL flask. After 2 h, ^1H NMR (CD_3CN) showed 4-*tert*-butylpyridinium trifluoroacetate and starting material (10%) with 90% [$Cp_2Mo_2(CO)_4$(MeOCH$_2$C≡CCH$_2$)][CF$_3$CO$_2$] [δ 8.46 (d, 2 H, ring, J = 5.8 Hz), 7.98 (d, 2 H, ring, J = 5.8 Hz), 5.54

(24) Prepared by the reaction of 2 MeI with LiOCH$_2$C≡CCH$_2$OLi (formed from HOCH$_2$C≡CCH$_2$OH and 2 MeLi in THF at −78 °C) at room temperature for 2 days.

(25) Wrighton, M. S.; Ginley, D. S. *J. Am. Chem. Soc.* **1975**, *97*, 4246–4251.

Table 1. Crystallographic Data for $Cp_2Mo_2(CO)_4(CH_2CCCH_2)(BF_4)_2(MeCN)_2$

formula	$C_{18}H_{14}B_2O_4F_8Mo_2{\cdot}2CH_3CN$
mol wt	741.91
color/shape	amber/parallelepiped
max crystal dimens, mm	0.34 × 0.20 × 0.20
temp, °C	−97
space group	$P\bar{1}$ (No. 2)
a, Å	9.779(1)
b, Å	10.982(3)
c, Å	12.680(3)
α, deg	103.09(2)
β, deg	93.04(2)
γ, deg	92.16(2)
V, Å^3	1322.8 (5)
Z	2
D_{calcd}, g cm^{-3}	1.862
μ_{calcd}, cm^{-1}	10.12
scan type	$\theta/2\theta$
2θ scan range, deg	5−55
range of h,k,l	+13,±15,±17
no. of reflns measd	8549
no. of reflns refined	5906
no. of params	419
GOF	1.26
R	0.0319
R_w	0.0524

(s, 2 H, CH_2^+), 5.26 (s, 10 H, Cp), 4.56 (s, 2 H, CH_2OMe), 3.37 (s, 3 H, Me), 1.37 (s, 9 H, CMe_3)]. Heating of the solution for 1 h at 50 °C had no effect on the product distribution.

Crystallography. Single crystals of **2**·[BF_4]$_2$(MeCN)$_2$ were grown from MeCN at −20 °C, mounted in thin-walled capillaries in air, and transferred to the cold stream of a Siemens R3m/v diffractometer (Mo Kα radiation (λ = 0.710 73 Å), graphite monochromator) equipped with a CT-2 low-temperature device at −97 °C. Lattice constants were determined by fine orientation of 25 reflections with 21.7° ≤ 2θ ≤ 27.7°. Intensities were measured in a conventional way using a variable scan rate and a 0.5 background/scan ratio.

All calculations were performed on a VAXStation 3500 computer using the SHELXTL PLUS software package.[26] After correcting for Lorentz and polarization effects, the structure was solved by direct methods. The structure was refined in a full matrix using difference Fourier techniques. After correcting for absorption,[27] all nonhydrogen atoms were allowed to refine anisotropically. Hydrogen atoms were allowed to refine isotropically with the exception of those on the molecules of the acetonitrile. The latter hydrogen atoms were placed in calculated positions (d_{C-H} = 0.96 Å).

X-ray structural details for **2**·[BF_4]$_2$(MeCN)$_2$ are given in Table 1. Final fractional coordinates and selected bond lengths and angles are given in Tables 2 and 3, respectively. The weighting scheme employed was $w^{-1} = \sigma^2(F_o) + 0.001288(F_o)^2$.

Results and Discussion

Synthesis and Structure of [$Cp_2Mo_2(CO)_4(CH_2CCCH_2)$][$BF_4$]$_2$ (2·[BF_4]$_2$). In the course of our studies of $Cp_2Mo_2(CO)_4$(alkyne) complexes as monomers for organometallic polymers, we discovered a new, one-step synthesis of **2**·[BF_4]$_2$ *via* protonation and dehydration of **1a** with $HBF_4{\cdot}Et_2O$ in CH_2Cl_2. The original method[21] involved conversion of **1a** to an intermediate monocation with aqueous HBF_4 and subsequent teatment with $(CF_3CO)_2O$ in CF_3CO_2H, followed by aqueous HBF_4. By our method, the product **2**·[BF_4]$_2$ precipitated as an orange-red semisolid which dried to an orange powder under vacuum. Recrystallization from MeCN produced large crystals of **2**•[BF_4]$_2$·2MeCN suitable for X-ray analysis.

(26) Siemens Analytical Intruments, Inc., Madison, WI, 1988.
(27) Walker, N.; Stuart, D. *Acta Crystallogr. Sect. A* **1983**, *39*, 158–166.

Table 2. Fractional Coordinates and Equivalent Isotropic Thermal Parameters (Å^2) for the Non-Hydrogen Atoms of $Cp_2Mo_2(CO)_4(CH_2CCCH_2)(BF_4)_2(MeCN)_2$

atom	x	y	z	U(eq),[a] Å^2
Mo1	0.16379(2)	0.72960(2)	0.33950(2)	0.01388(8)
Mo2	0.37094(2)	0.78745(2)	0.18560(2)	0.01369(8)
C1	0.0246(3)	0.7070(3)	0.2117(2)	0.0204(8)
O1	−0.0506(2)	0.6923(2)	0.1393(2)	0.0296(7)
C2	0.0813(3)	0.5655(3)	0.3639(2)	0.0229(8)
O2	0.0317(2)	0.4794(2)	0.3817(2)	0.0328(7)
C3	0.5500(3)	0.7057(3)	0.1412(2)	0.0219(8)
O3	0.6484(2)	0.6620(2)	0.1161(2)	0.0325(7)
C4	0.4820(3)	0.8804(2)	0.3211(2)	0.0200(8)
O4	0.5448(2)	0.9285(2)	0.3969(2)	0.0279(7)
C5	0.0789(3)	0.7998(3)	0.5107(2)	0.0260(9)
C6	−0.0073(3)	0.8355(3)	0.4306(2)	0.0247(9)
C7	0.0703(3)	0.9199(3)	0.3843(2)	0.0222(8)
C8	0.2040(3)	0.9373(2)	0.4369(2)	0.0193(8)
C9	0.2092(3)	0.8614(3)	0.5145(2)	0.0226(8)
C10	0.2075(3)	0.8873(3)	0.1004(3)	0.0250(9)
C11	0.2938(3)	0.9797(3)	0.1744(2)	0.0250(9)
C12	0.4282(3)	0.9714(3)	0.1360(2)	0.0244(9)
C13	0.4241(3)	0.8756(3)	0.0411(2)	0.0243(9)
C14	0.2888(3)	0.8243(3)	0.0184(2)	0.0245(9)
C15	0.3805(3)	0.6483(3)	0.3940(2)	0.0205(8)
C16	0.3691(3)	0.6572(2)	0.2875(2)	0.0167(7)
C17	0.2606(3)	0.6112(2)	0.2102(2)	0.0168(7)
C18	0.2682(3)	0.5780(2)	0.0990(2)	0.0204(8)
B1	0.7992(3)	0.9982(3)	0.1869(3)	0.025(1)
F1	0.7371(2)	0.9382(2)	0.0868(2)	0.0394(7)
F2	0.7372(2)	1.1094(2)	0.2240(2)	0.0438(7)
F3	0.9388(2)	1.0202(2)	0.1766(2)	0.0480(8)
F4	0.7835(2)	0.9234(2)	0.2604(2)	0.0374(7)
B2	−0.3049(4)	0.7345(3)	0.5834(3)	0.031(1)
F5	−0.1847(2)	0.8004(2)	0.6314(2)	0.0331(6)
F6	−0.4137(2)	0.8150(2)	0.6007(2)	0.0376(6)
F7	−0.2917(3)	0.6948(3)	0.4730(2)	0.069(1)
F8	−0.3307(3)	0.6357(2)	0.6302(3)	0.073(1)
N1	0.5170(4)	0.3893(3)	0.1322(3)	0.048(1)
C19	0.5791(4)	0.3939(3)	0.2119(3)	0.032(1)
C20	0.6573(4)	0.3994(3)	0.3138(3)	0.041(1)
N2	−0.0551(3)	0.3978(3)	0.1255(3)	0.026(1)
C21	0.0314(4)	0.3337(3)	0.1220(2)	0.033(1)
C22	0.1452(4)	0.2479(3)	0.1170(3)	0.046(1)

[a] Equivalent isotropic U defined as one-third of the trace of the orthogonalized U_{ij} tensor.

Table 3. Selected Bond Lengths (Å) and Angles (deg) for $Cp_2Mo_2(CO)_4(CH_2CCCH_2)(BF_4)_2(MeCN)_2$

(a) Bond Lengths

Mo1−Mo2	3.0330(3)	C16−C17	1.402(3)
Mo1−C15	2.456(3)	Mo2−C18	2.464(2)
Mo1−C16	2.263(2)	Mo2−C17	2.272(2)
Mo1−C17	2.137(2)	Mo2−C16	2.134(2)
C15−C16	1.376(3)	C17−C18	1.381(3)

(b) Bond Angles

C15−C16−C17	127.2(2)	C16−C17−C18	126.6(2)
Mo1−C17−C18	144.4(2)	Mo2−C16−C15	143.1(2)
Mo1−C17−C16	76.4(1)	Mo2−C16−C17	76.9(1)
Mo1−C17−Mo2	86.88(8)	Mo2−C16−Mo1	87.18(9)
Mo1−C1−O1	178.2(2)	Mo2−C3−O3	179.1(2)
Mo1−C2−O2	176.1(2)	Mo2−C4−O4	177.8(2)

Scheme 1

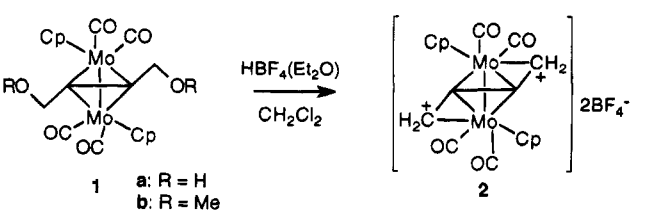

1 a: R = H b: R = Me 2

The molecular structure and numbering scheme are shown in Figure 1. Positional parameters and selected bond lengths and angles are given in Tables 2and 3. The

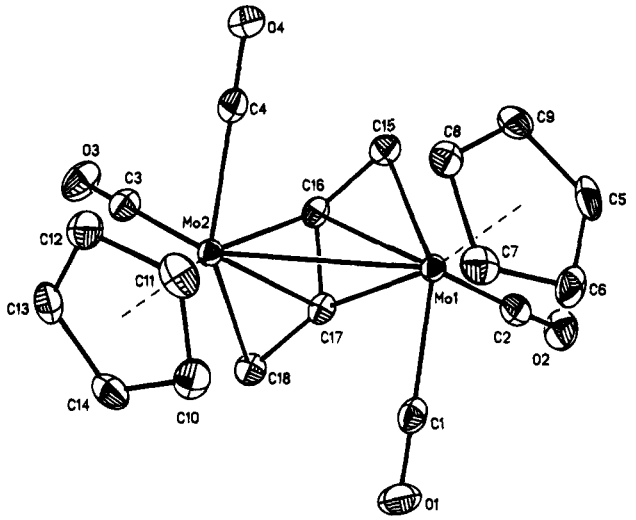

Figure 1. ORTEP view of the cation in **2**·$[BF_4]_2$ (ellipsoids drawn at 50% probability).

Table 4. Selected Bond Lengths (Å) and Angles (deg) for $[Cp_2Mo_2(CO)_4(HCCCR^1R^2)][BF_4]$ (3a–c)

	R^1	R^2	Mo–Mo	Mo–C^+	HC–C	C–C^+	C–C–C
3a[a]	H	H	3.021(1)	2.439(6)	1.353(8)	1.347(8)	136.4(6)
3b[b]	H	Me	3.007	2.613	1.395(10)	1.380(9)	130.5(7)
3c[a]	Me	Me	2.982(2)	2.75(1)	1.39(2)	1.38(2)	136(1)

[a] Reference 12. [b] Reference 13.

Scheme 2

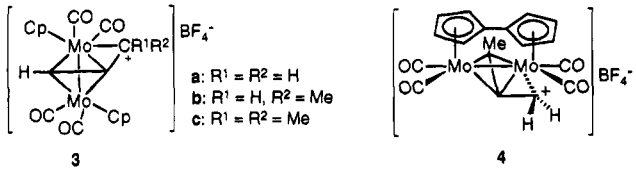

BF_4^- counterions and MeCN trapped in the lattice do not interact with the dication. The molecular symmetry is nearly C_2 with the bridging C_4H_4 ligand adopting a μ-η^3,η^3 coordination mode.

The series of analogous metal-stabilized monocarbenium ions, $[Cp_2Mo_2(CO)_4(\mu\text{-}\eta^2,\eta^3\text{-}HCCCR_1R_2)][BF_4]$ (**3a** $R^1 = R^2 = H$; **3b** $R^1 = H$, $R^2 = Me$; **3c** $R^1 = R^2 = Me$), has been structurally characterized previously (see Table 4 for selected bond angles and distances). Compounds **3a–c** all have semibridging CO ligands, whereas **2** has only terminal CO ligands (∠M–C–O = 176–179°), as also indicated by the absence of CO stretching bands in the bridging region. The Cp ligands in **2** are in a *syn* orientation having an acute torsional angle (∠Cn1–Mo1–Mo2–Cn2 = 60.9°) (Cn = ring centroid). With respect to steric crowding around the metal centers, **2** most resembles $[FvMo_2(CO)_4(\mu\text{-}\eta^2,\eta^3\text{-}MeCCCH_2)][BF_4]$ (Fv = fulvalene) (**4**)[10] in which terminal CO ligands result from having the "Cp" ligands linked together.

In going from **3a** to **3c**, the combined effects of increasing steric crowding and decreasing electrophilicity at the "carbenium" center result in a progressively weaker Mo–C^+ interaction as hydrogen atoms are substituted by methyl groups. As expected, the stronger the Mo–C^+ interaction, the longer the Mo–Mo bond. The strong stabilization of the dicarbenium ion by both metals in **2** (Mo1–C15 = 2.456 (3) Å, Mo2–C18 = 2.464(2) Å) results in a slightly longer Mo–Mo bond length (3.0330(3) Å) than in **3a–c**, but the Mo–Mo distance is still consistent with a single bond between the atoms. The C–C bond distances of the alkyne-derived ligand in **2** are all essentially equal, and the C–C–C angles in **2** are significantly smaller (127.2(2)°, 126.6(2)°) than those in **3a–c** (130.5–136.4°).

Scheme 3

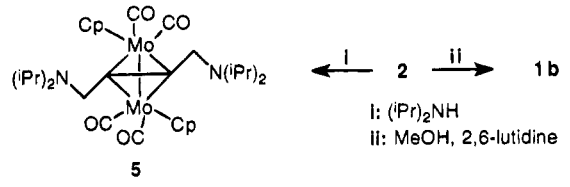

Scheme 4

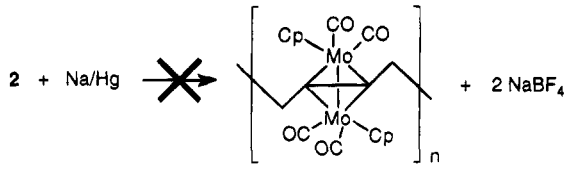

Reactivity of $[Cp_2Mo_2(CO)_4(CH_2CCCH_2)][BF_4]_2$ (2·$[BF_4]_2$). The monocations, $Cp_2M_2(CO)_4(\mu\text{-}HCCCH_2^+)$ (M = Mo, W), have been shown[4,10,11,13,15,17,28] to react with a variety of nucleophiles (Nu) to give $Cp_2M_2(CO)_4(\mu\text{-}HC{\equiv}CCH_2Nu)$ or with Na/Hg to yield radicals which dimerize by C–C coupling of the methylene groups.[4,13] Reutov et al.[21] reported the hydrolysis of **2**·$[BF_4]_2$ back to **1a** and its reduction with $NaBH_4$ to give $Cp_2Mo_2(CO)_4(\mu\text{-}MeC{\equiv}CMe)$.

We have found that **2**·$[BF_4]_2$ reacts in neat diisopropylamine to give clean conversion to the bis(amine) product **5**. Four equivalents of amine was required, as the proton was scavenged as $[(^iPr)_2NH_2][BF_4]$. Secondary amines have been shown to add to monocarbenium ions stabilized by either Mo[29] or Co.[5,29a] Neat anhydrous MeOH failed to convert **2**·$[BF_4]_2$ to **1b**, but the addition of 2,6-lutidine produced an immediate color change to bright red, signaling that addition had taken place. El Amouri et al.[30] found that $[Co_2(CO)_6(HCCCH_2)][BF_4]$ was readily converted to $Co_2(CO)_6(HC{\equiv}CCH_2OMe)$ in neat MeOH. The decreased reactivity of **2**·$[BF_4]_2$ results from the greater stabilization of a carbenium ion by Mo than by Co. Gruselle *et al.*[29a] have shown that the equilibrium constants in MeOH for the $[M_2L_6(HC{\equiv}CCH_2)][BF_4]$ cations (M_2L_6 = $Co(CO)_3$, $MoCp(CO)_2$) differ by 10 orders of magnitude. That monocarbenium ions are preferentially stabilized by the Mo center of mixed metal systems (M_2L_6 = $CoMoCp(CO)_5$) was revealed by variable temperature NMR,[6] rationalized by EHMO calculations, and recently demonstrated crystallographically.[14]

The reduction of **2** was attempted in hopes of making a polymer having Mo_2C_2 clusters in the chain. An intractable mixture was formed when **2** was allowed to react with Na/Hg, and no polymer or oligomers were detected. Similar reductive dimerization reactions[4,13]

(28) (a) Sokolov, V. I.; Barinov, I. V.; Reutov, O. A. *Izv. Akad. Nauk SSSR, Ser. Khim.* **1982**, *31*, 1922. (b) Barinov, I. V.; Sokolov, V. I.; Reutov, O. A. *Zh. Org. Khim.* **1986**, *22*, 2457–2458.

(29) (a) Gruselle, M.; Philomin, V.; Chaminant, F.; Jaouen, G.; Nicholas, K. M. *J. Organomet. Chem.* **1990**, *399*, 317–326. (b) Barinov, I. V.; Chertov, V. A.; Reutov, O. A. *J. Organomet. Chem.* **1993**, *455*, C9.

(30) El Amouri, H.; Gruselle, M.; Jaouen, G.; Daran, J. C.; Vaissermann, J. *Inorg. Chem.* **1990**, *29*, 3238–3242.

Scheme 5

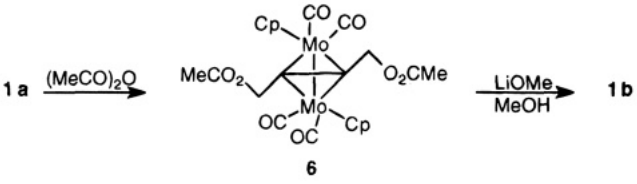

Scheme 6

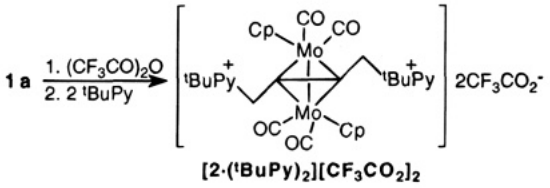

Scheme 7

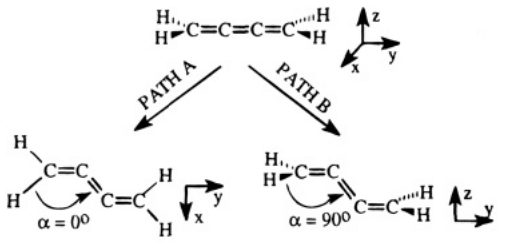

of monocations gave mixtures that required chromatography for purification, but the C—C coupled dimers were isolated in moderate yield.

To avoid the extreme moisture sensitivity and solution instability of **2**·$[BF_4]_2$, we attempted to synthesize masked dicarbenium ions $Cp_2Mo_2(CO)_4(XCH_2C{\equiv}CCH_2X)$ with good leaving groups ($X = Cl^-$, $CH_3CO_2^-$, $CF_3CO_2^-$). Reaction of $ClCH_2C{\equiv}CCH_2Cl$ with $Cp_2Mo_2(CO)_4$ resulted in chlorination of the metal. The soluble portion of the reaction mixture was mostly $CpMo(CO)_3Cl$, as identified by its IR spectrum[25] and its singlet in the ^1H NMR spectrum. Reaction of **1a** with acetic anhydride cleanly yielded the diester (**6**) in good yield. Limited substitution for acetate was possible. With LiOMe in MeOH, almost 90% **1b** was obtained. Only a 75% yield of $Cp_2Mo_2(CO)_4(PhCO_2CH_2C{\equiv}CCH_2O_2CPh)$ was obtained by the reaction of benzoic acid and **6**.

Reaction of **1a** with trifluoroacetic anhydride yielded an oily, orange diester (**2**·$[CF_3CO_2]_2$) which was ionic in MeCN solution. Addition of a coordinating base, 4-*tert*-butylpyridine (^{t}BuPy), allowed the isolation of a solid adduct, $[Cp_2Mo_2(CO)_4(({}^t\text{BuPy})CH_2C{\equiv}CCH_2({}^t\text{BuPy}))][CF_3CO_2]_2$ (**2**·$({}^t\text{BuPy})_2[CF_3CO_2]_2$), which could be monosubstituted by −OMe in neat MeOH. Complete conversion to **1b** could not be effected due to the strong stabilization of the carbenium ion by 4-*tert*-butylpyridine. El Amouri et al.[30] found $[Co_2(CO)_6(HC{\equiv}CCH_2L)][BF_4]$ would not react with MeOH with L = pyridine, but substitution was facile with L = R_2S.

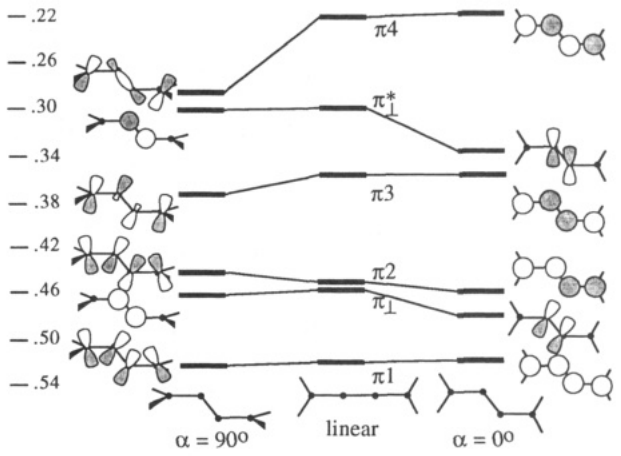

Figure 2. Fragment molecular orbitals (FMOs) of the C_4H_4 ligand as a function of the kink distortion. The energy scale is in Hartrees.

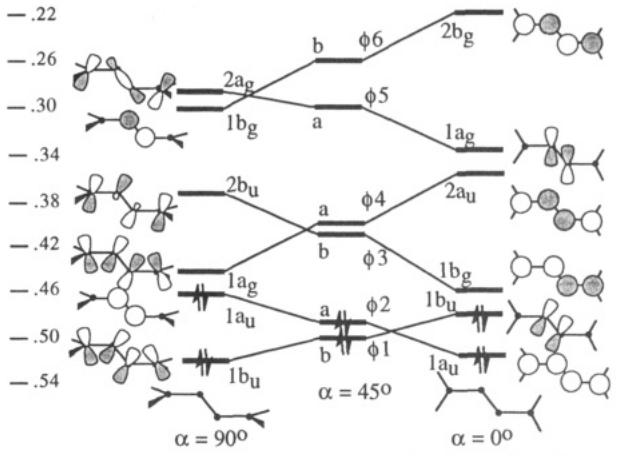

Figure 3. Fragment molecular orbitals of the C_4H_4 ligand as a function of the HCCC dihedral angle, α. The energy scale is in Hartrees.

EHMO Analysis: $Cp_2Mo_2(CO)_4$ Fragment MOs (FMOs). The dication **2** may be constructed from triply-bonded $Cp_2Mo_2(CO)_4$ ("M_2") and $C_4H_4^{2+}$ fragments. The $Cp(CO)_2Mo$ unit is an example of an ML_5 fragment whose frontier orbitals consist of the σ spd hybrid, a pair of d_{xz}, d_{yz} π-symmetry orbitals, and the δ-symmetry d_{xy}.[31] Combinations of these FMOs in an $L_5M{-}ML_5$ dimer gives rise to a $\sigma\pi\delta\delta^*\pi^*\sigma^*$ set of MOs. A d^5 metal ion, e.g., Mo(I) then produces a $\sigma^2\pi^4\delta^2\delta^{*2}$ configuration, i.e., a formal M≡M triple bond.

The presence of the low-lying π^* MOs confers on the Mo≡Mo triple bond a high reactivity toward nucleophiles, as shown schematically in eq 1.[32,33]

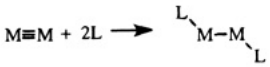

(1)

The net addition of four electrons in reactions, e.g., eq 1, effectively fills the π^* orbitals, and the M—M bond order is reduced to unity. The two orthogonal π-MOs of the bridging acetylene ligand can donate the requisite four electrons, hence the ready formation of the tetrahedrane-type clusters, $Cp_2Mo_2(CO)_4(RC{\equiv}CR)$.

(31) Hoffmann, R. *Angew. Chem., Int. Ed. Engl.* **1982**, *21*, 711.
(32) Curtis, M. D.; Messerle, L.; Fotinos, N. A.; Gerlach, R. F. *ACS Symp. Ser.* **1981**, *155*, 221.
(33) Winter, M. J. *Adv. Organomet. Chem.* **1989**, *29*, 101.

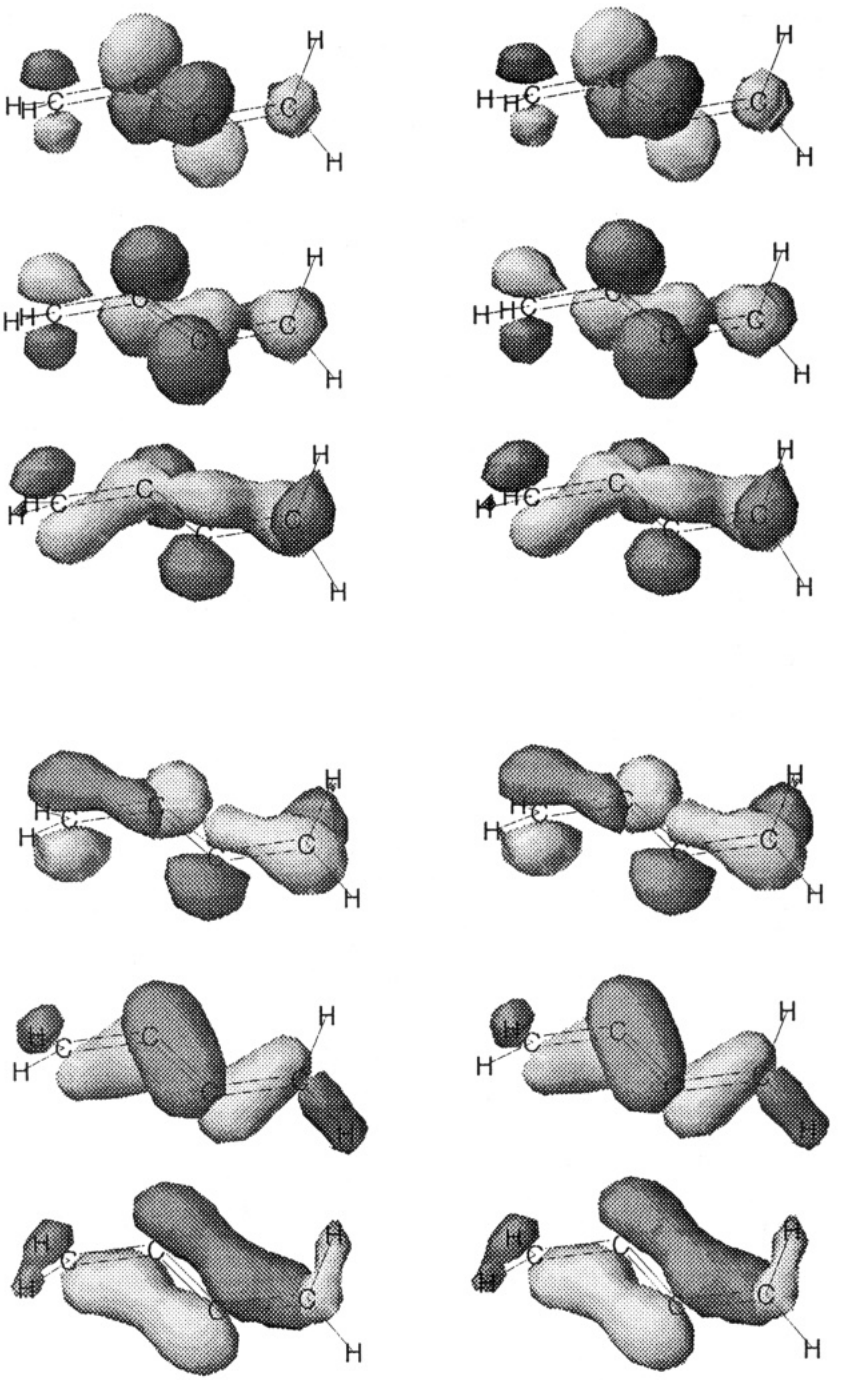

Figure 4. Stereoviews of the frontier orbitals, $\phi 1-\phi 6$, of the C_4H_4 ligand. The orbitals are ordered from lowest energy ($\phi 1$) at the bottom to highest energy ($\phi 6$) at the top.

In the actual $Cp(CO)_2Mo$ fragment, the FMOs are considerably distorted from the axially symmetric ML_5 picture because of the disparity in π-acceptor ability between the Cp and CO ligands. Furthermore, the energies and makeup of the metal–metal MOs in the $Cp_2Mo_2(CO)_4$ dimer depend critically on the Mo–Mo–Cp and Mo–Mo–CO angles as well as on the Cp–Mo–Mo–Cp dihedral angle.[34,35] The relative orientation of the $Cp(CO)_2Mo$ units in the M_2 dimer as found in dication **2** is such that the $Cp_2Mo_2(CO)_4$ dimer approaches C_2 symmetry with the C_2 axis perpendicular to the Mo–Mo bond and bisecting the Cp–Mo–Mo–Cp dihedral angle. In this low symmetry, the axially defined labels, σ, π, and δ, lose their strict meaning and the resulting MOs often appear to be mixtures of $\sigma + \delta$, $\pi^* + \delta^*$, etc. The rather complex shaped frontier FMOs of the M_2 fragment are given in stereoviews in the supplementary material.

C_4H_4 FMOs. The organic, C_4H_4 fragment with the geometry found in dication **2** can be derived by distortions of the linear butatriene molecule, as shown in Scheme 7. In path A, the C_4 skeleton is kinked in the xy plane and the $C_2(z)$ axis of the D_{2h} point group is maintained. The resultant structure is planar and belongs to the C_{2h} point group, and the HCCC dihedral angle (α) is zero. In path B, the kink is in the yz plane; the $C_2(x)$ axis of D_{2h} is maintained to give a C_{2h} structure in which the HCCC dihedral, α, is 90°.

(34) (a) Jemmis. E. D.; Pinhas. A. R.; Hoffmann, R. *J. Am. Chem. Soc.* **1980**, *102*, 2576. (b) Morris-Sherwood, B. J.; Powell, C. B.; Hall, M. B. *J. Am. Chem. Soc.* **1984**, *106*, 5079.

(35) Curtis, M. D. *Polyhedron* **1987**, *6*, 759.

Table 5. Bond Orders, Atomic Charges, and Total Energies for Different Structures of the $C_4H_4^{n+}$ (n = 0, 2) Ligand

	linear (triene)	kinked α = 0°	kinked α = 45°	kinked α = 90°
		$n = 0$		
C_α–C_β	1.85	1.83	1.75	1.78
C_β–C_γ	2.06	1.96	2.03	2.03
q_α	−0.07	−0.08	−0.10	0.02
q_β	−0.04	−0.03	−0.02	−0.13
E_T (au)	−13.00	−12.95	−12.90	−12.92
		$n = 2$		
C_α–C_β	1.25	1.23	1.53	1.23
C_β–C_γ	2.37	2.26	1.87	2.31
q_α	0.66	0.66	0.47	0.70
q_β	0.23	0.24	0.38	0.18
E_T (au)	−12.08	−12.04	−12.07	−12.05

The effects of these distortions on the MOs of butatriene are instructive. The MOs of D_{2h} butatriene are the familiar π_1–π_4 butadiene-like MOs on which are superimposed $\pi_\perp$ and $\pi_\perp$* MOs derived from the orthogonal p-orbitals on C_2 and C_3 (the two central carbon atoms). Kinking the C_4 chain in the xy-plane has little effect on π_1–π_4 since the p-orbital interactions are being rotated about their local symmetry axes, i.e., the local z-axes. However, $\pi_\perp$ and $\pi_\perp$* are mixed with σ(CC) and σ(CH) type MOs (Figure 2). The opposite result is obtained when the kink is about $C_2(x)$. Now $\pi_\perp$ and $\pi_\perp$* are essentially unperturbed, and π_1–π_4 are distorted as shown in Figure 2.

These conformational isomers, obtained by kinking a linear butatriene molecule, can be interchanged by rotations of the methylene groups about the C–C bonds. These rotations are described by the dihedral angle α, and when α = 45° an identical structure is arrived at from the two paths, A and B. Hence, the MOs must correlate as shown in Figure 3. Note that as α moves away from 0 or 90° (C_{2h} symmetry), close lying MOs with the same rotational symmetry but opposite inversion symmetry mix to give high- and low-energy combinations in which the $\pi_{||}$ and $\pi_\perp$ character are interchanged. This leads to extensive mixing of the "σ" and "π" orbitals at intermediate twist angles, 0° < α < 90°, and accounts for the odd Möbius striplike appearance of some of the frontier orbitals, ϕ_1–ϕ_6 of the C_4H_4 ligand in dication **2** (Figure 4).

Table 5 documents the changes in bond order and atomic charges as a function of the kink and twist distortions. For the neutral molecule, the linear triene structure is calculated to have the lowest energy, as expected, and the C–C bond orders are as expected for C=C double bonds. In the $C_4H_4^{2+}$ dication, the linear structure still has the lowest calculated energy of the three considered, but the α = 45° structure is only 0.01 au higher in energy. The C_4H_4 structure as found in dication **2** has a further distortion: a slight bend at right angles to the kink, and the calculated energy of the $C_4H_4^{2+}$ fragment with the crystal coordinates is −12.11 au, i.e., slightly lower than that of the linear structure. This observed structure also has the largest HOMO–LUMO gap (Figures 2 and 3) and is likely to be the most stable structure for the singlet states considered here.

In any event, the kinked and twisted structure has the effect of distributing the positive charge over the entire C_4 chain; q_α = +0.47 and q_β = +0.38 *vis-à-vis* q_α ~ +0.7 and q_β ~ +0.2 in the other three structures. Thus, even without coordination to the metal, the positive charge is dispersed in the distorted C_4H_4 structure, and it appears that the conformation of the C_4 ligand in complex **2** is close to the preferred structure of an isolated $C_4H_4^{2+}$ singlet state molecule.

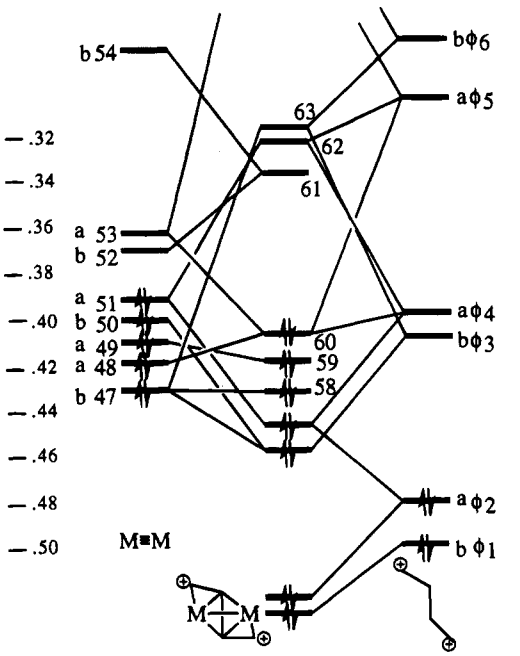

Figure 5. MO energy level diagram of dication **2**. The energy scale is in Hartrees.

$M_2(C_4H_4)^{2+}$ and $M_2(C_3H_3)^+$ Molecules. The $Cp_2Mo_2(CO)_4$ and $C_4H_4^{2+}$ FMOs combine to form the frontier MOs of the dication **2**, as indicated by the energy level diagram in Figure 5. All the low-lying C_4H_4 FMOs find a good overlap match with the metal FMOs and form a nest of four M–C bonding MOs that reflects the strong bonding between the Mo atoms and each of the carbon atoms of the C_4H_4 ligand. Above the set of M–C bonding orbitals are three MOs, **58**–**60**, that are shown in stereo in Figure 6. MO **60** is derived from a δ_{MM} orbital and several C_2-symmetric C_4-ligand FMOs. This orbital is primarily nonbonding but has Mo–C_β bonding character (C_α are the methylene carbon atoms at the ends of the C_4 chain). MO **59** is clearly MM σ-bonding; MO **58** is MM nonbonding but possesses M–CO bonding character. MO **58** is derived from a highly distorted δ_{MM} orbital.

The low-lying empty MOs, **61**–**63**, are shown in Figure 7. Orbital **61** has σ_{MM}* character but is mainly M–CO π-bonding. MOs **62** and **63** have substantial contributions from atomic orbitals located on the terminal methylene carbon atoms of the C_4H_4 ligand. These MOs are complementary in the sense that MO **63** is spread over Mo2, C18, and a carbonyl group, while MO **62** is delocalized over Mo1, C15, and the symmetry-related carbonyl group. The computed bond orders and atomic charges are listed in Table 6.

It is interesting to compare the calculations for **2** with those for the monocationic complex, $Cp_2Mo_2(CO)_4(HCCCH_2)^+$, **3a**$^+$. The MOs of the $C_3H_3^+$ ligand are the π_1–π_3 allyl group-like orbitals and the $\pi_\perp$ and $\pi_\perp$* MOs are formed by the two orthogonal p-orbitals. The nonbonding allyl-like orbital, π_2, lies closest in energy to the d-orbital manifold of the Mo_2 fragment and forms strong bonding and antibonding combinations with metal–metal π*/δ* orbitals. The antibonding combina-

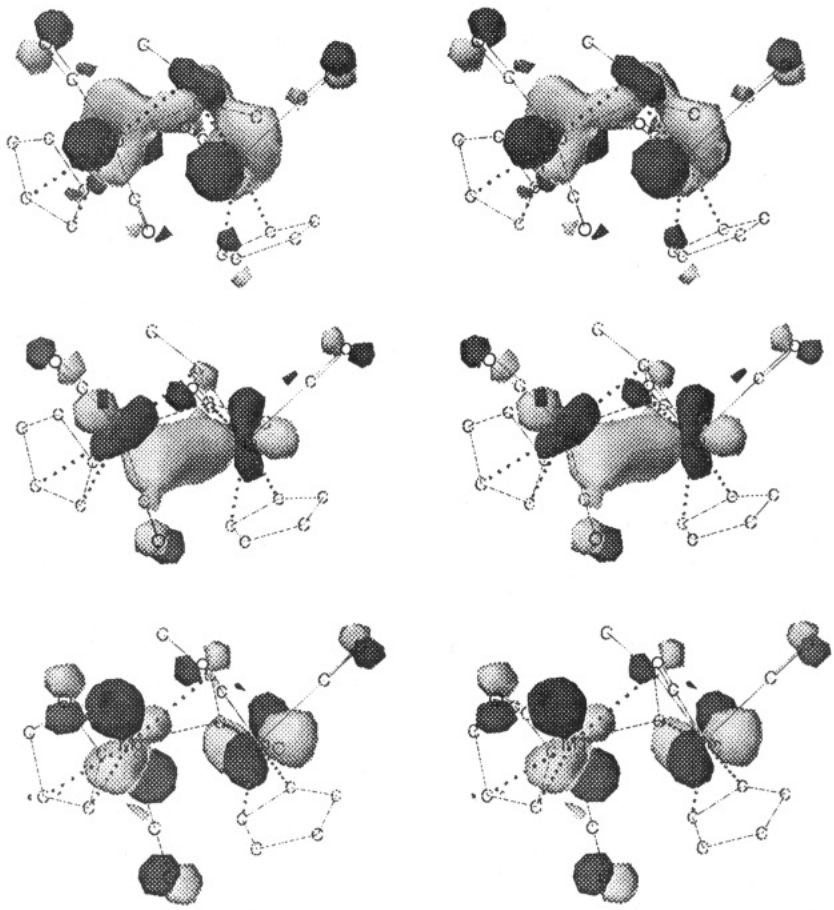

Figure 6. Stereoviews of MOs **58**–**60** of dication **2**. As in Figure 4, increasing energy is from bottom to top.

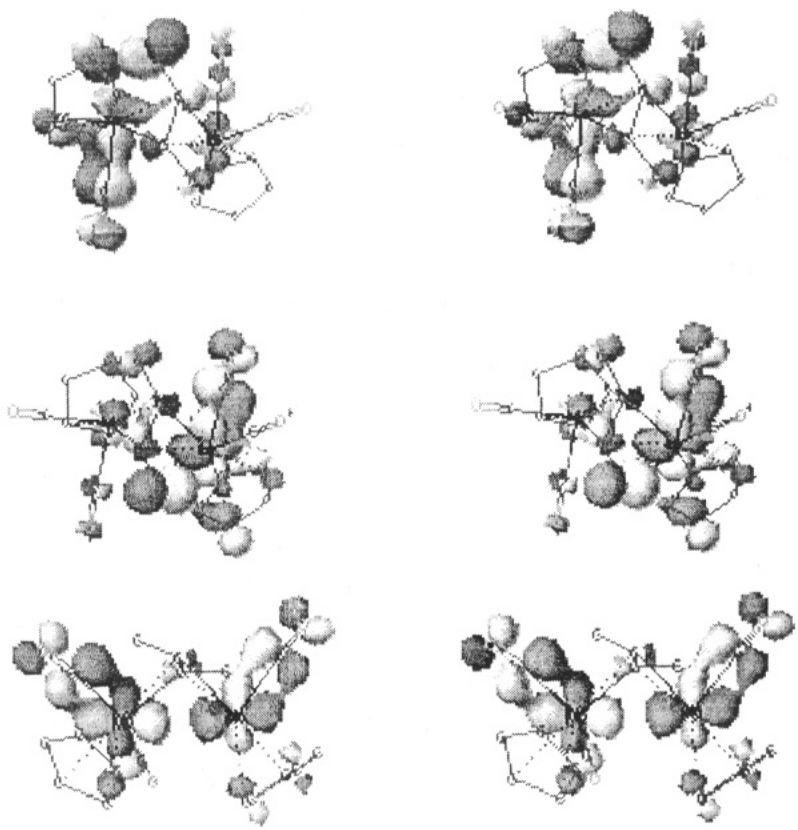

Figure 7. Stereoviews of MOs **61**–**63** of dication **2.** As in Figure 4, increasing energy is from bottom to top.

tion forms the LUMO of the molecule, shown in Figure 8, and has substantial M—CO bonding character as well as significant contributions from atomic orbitals on the terminal carbon atoms of the C_3H_3 ligand. The calcu-

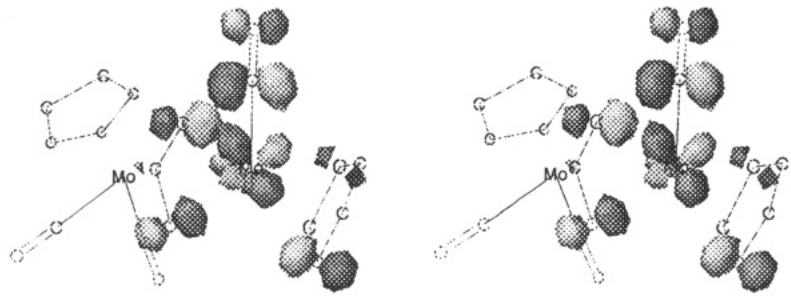

Figure 8. Stereoview of the LUMO (MO **65**) of monocation **3a**.

Table 6. Bond Orders and Atomic Charges for Dication 2 and Monocation 3a

	dication **2**	monocation **3a**
	Bond Orders[a]	
Mo—Mo	0.50	0.40
C_α—C_β	1.40	1.38
C_β—C_γ	1.26	1.40
M—C_α	0.50	0.49[c] (0.03)[d]
M—C_β	0.29	0.28[c] (0.69)[d]
M—C_γ	0.78	0.62[c] (0.65)[d]
	Atomic Charges	
Mo1[b]	+1.02	+0.98
Mo2	+1.02	+0.76
C_α	−0.24	−0.13
C_β	−0.13	−0.06
C_γ	−0.13	−0.32

[a] C_α refers to the methylene carbon of the bridging hydrocarbyl ligand, C_β is adjacent to C_α, and C_γ is adjacent to C_β. [b] Mo1 is bonded to C_α in the monocation, **3a**. [c] Mo1—carbon bond orders. Mo1 is bonded to the $-CH_2$ group. [d] Mo2—carbon bond orders.

lated bond orders and atomic charges are also listed in Table 6. The bonding in **3a** has been described[4] as a μ-η^2,η^3-allylic structure in which the Mo2—C bonds take the place of C—H bonds in a mononuclear π-allyl complex. The bond orders reported in Table 6 support this description. Mo2 is strongly bonded to C_β and C_γ, while Mo1 is bonded most strongly to the terminal carbon atoms, C_α and C_γ. The latter pattern is characteristic of mononuclear π-allyl metal bonding.[4] The C—C bond orders are about equal, as expected for a π-allyl formulation.

In the dication, **2**, there is near C_2 symmetry and the bonding between the C_4 ligand and each of the metals is equivalent. The bonding to C_γ is again the strongest, followed by the Mo—C_α interaction. There is a greater disparity in the C—C bond orders than was present in **3a**. The C_α—C_β bond order is 1.40 as compared to 1.26 for the C_β—C_γ bond.

In both compounds, **2** and **3a**, carbon atoms of the "cationic" ligand are calculated to have *negative* charge. Thus, complexation to the dimetal center effectively quenches the carbenium ion character of the ligand and most of the positive charge is transferred to the metal atoms. This conclusion is consistent with the observed increase of over 100 cm^{-1} in the ν_{CO} stretching frequencies of the dication, as compared to those of the alkyne complex precursors.

Chemical Regioselectivity. It is experimentally established that nucleophiles attack **2** and **3a** at the methylene group to give complexes of substituted alkynes. Since the methylene groups are negatively charged, the implication is that the addition reaction is either frontier orbital controlled or is reversible so that the thermodynamically most stable product is formed. The LUMO of **3a** is clearly capable of directing a ligand to the methylene group, although there is also significant latent reactivity at C_γ. Addition at C_γ would give a μ-η^2,η^2-propadiene (allene) complex, examples of which are known.[4,36] If followed at all, this reaction path must be reversible since nucleophilic addition to cations derived from allenes gives alkyne complexes.[4] The FMOs and ligand charges are very similar to those governing nucleophilic attack at coordinated π-allyl groups in cationic complexes, $L_nM(C_3H_5)^+$.[37]

The situation with the "dicarbenium" complex, **2**, is not so straightforward. The LUMO is primarily M—CO π-bonding and M—M antibonding. Upon reduction of **2**, the added electron would be expected to occupy this orbital. Since this orbital places no electron density on the C_4H_4 ligand, it is not surprising in light of this result that reduction of **2** does not lead to C—C coupled products, as does reduction of **3a**.[4]

Nucleophilic adduct formation is different from one-electron reduction. The metal centers in **2** are well shielded by the shell of ligands. MO **62** provides an alternative, relatively unhindered acceptor site at one of the methylene carbon atoms. Eventual attack of the nucleophile at this position leads to a stable complex whose electronic structure would closely resemble that of **3a**; i.e., the LUMO is now concentrated on the bridging ligand. A second addition takes the complex to the final μ_2-(η^2-alkyne) type complex.

Conclusions

The bonding in dication **2** is very similar to that in the monocation complexes, e.g., $Cp_2Mo_2(CO)_4(C_3H_3)^+$. The electron distribution is consistent with the previously suggested model that depicts the bridging ligand as a π-allyl ligand to one metal with the other metal bonded to the perpendicular π-orbital of the alkyne fragment. Most of the positive charge accrues on the metal and carbonyl carbon atoms. In fact, the calculations suggest that the carbon atoms of the bridging "carbenium" ion actually carry a negative charge. Nucleophilic addition to these cationic complexes is therefore frontier orbital controlled. Differences in the nature of their respective LUMOs can account for the different behavior of **2** and monocations toward one-electron reduction.

Acknowledgment. We are grateful to the donors of the Petroleum Research Fund, administered by the American Chemical Society, and to the National Science Foundation (CHE-8619864) for generous financial support.

(36) Bailey, W. I., Jr.; Chisholm, M. H.; Cotton, F. A.; Rankel, L. A. *J. Am. Chem. Soc.* **1978**, *100*, 802.
(37) Curtis, M. D.; Eisenstein, O. *Organometallics* **1984**, *3*, 887.

Table 7. Atomic Parameters Used in the EHMO Calculations

orbital		H_{ii} (eV)	ζ1	ζ2	C1	C2
H	1s	−13.60	1.300			
C	2s	−21.40	1.625			
	2p	−11.40	1.625			
O	2s	−28.48	2.192			
	2p	−13.62	2.018			
Mo	5s	−8.77	1.960			
	5p	−5.6	1.900			
	4d	−11.06	4.540	1.900	0.5899	0.5899

Appendix

Extended Huckel molecular orbital (EHMO) calculations were performed with the Personal CAChe software system running on a Macintosh Centris 650. Plotting of the MOs was also accomplished with the software system. The atomic parameters used in the calculations are collected in Table 7. The atomic coordinates were obtained directly from the crystal fractional coordinates.

Supplementary Material Available: Tables of crystallographic statistics, H-atom positional and thermal parameters, anisotropic thermal parameters for non-H atoms, bond distances, and bond angles for **2**, an MO energy level diagram for **3a**, and stereofigures of the $Cp_2Mo_2(CO)_4$ fragment MOs (12 pages). Ordering information is given on any current masthead page.

OM940395T